Innovative Systems Design and Engineering www.iiste.org
ISSN 2222-1727 (Paper) ISSN 2222-2871 (Online)
Vol 2, No 6, 2011

Design of Multilevel Inverter Driven Induction Machine

Urmila Bandaru
G.. Pulla Reddy Engineering College, Kurnool
A.P., India
E-mail: urmila913@gmail.com

Subbarayudu
Brindavan Institute of Technology, Kurnool
A.P., India
E-mail: dsr@gmail.com

The research is financed by Asian Development Bank. No. 2006-A171(Sponsoring information)

Abstract

Multilevel inverters have gained interest in recent years in high-power medium-voltage industry. This paper considered the most popular structure among the transformer-less voltage source multilevel inverters, the diode-clamped inverter based on the neutral point converter. This paper proposes a single carrier multi-modulation SVPWM technique with conventional space vector switching sequence. Simulation results presents comparison of single and multicarrier conventional space vector switching sequence with general switching sequence of nine-level diode-clamped inverter for stator currents, electromagnetic torque and speed for constant modulation index and for constant V/f control method. Simulation is carried out in MATLAB-Simulink software.

Keywords- Multilevel inverter, APODC, SVPWM, total harmonic distortion, Diode-clamped inverter, SCMMOS, MCMMOS, Induction machine, synchronously rotating reference frame

1. Introduction

Multilevel inverters have drawn tremendous interest in high-power medium-voltage industry. In literature, inverters with voltage levels three or more referred as multilevel inverters. The inherent multilevel structure increase the power rating in which device voltage stresses are controlled without requiring higher ratings on individual devices. They present a new set of features that suits well for use in static reactive power compensation, drives and active power filters. Multilevel voltage source inverter allows reaching high voltages with low harmonics without use of series connected synchronized switching devices or transformers. As the number of voltage levels increases, the harmonic content of output voltage waveform decreases significantly. The advantages of multilevel inverter are good power quality, low switching losses, reduced output dv/dt and high voltage capability. Increasing the number of voltage levels in the inverter increases the power rating. The three main topologies of multilevel inverters are the Diode clamped inverter, Flying capacitor inverter, and the Cascaded H-bridge inverter by Nabae et al. (1981).

The PWM schemes of multilevel inverters are Multilevel Sine-Triangle Carrier Pulse Width Modulation-SPWM and Space Vector Pulse Width Modulation-SVPWM. Multilevel SPWM involves comparison of reference signal with a number of level shifted carriers to generate the PWM signal. Due to its simplicity and its well defined harmonic spectrum which is concentrated at the carrier frequency, its sidebands, and its multiples with their sidebands, the SPWM method has been utilized in a wide range of AC drive applications. However, the method has a poor voltage linearity range, which is at most 78.5 % of the six-step voltage fundamental component value, hence poor voltage utilization. Therefore, the zero sequence signal injection techniques that extend the SPWM linearity range have been introduced for isolated neutral load applications which comprise the large majority of AC loads. The carrier based PWM methods can operate with high switching frequency and offer high waveform quality and implementation advantages. Carrier based PWM methods employ the per carrier cycle volt-second balancing principle to program a desirable inverter output voltage waveform. The programmed PWM technique, SVPWM involves synthesizing the reference voltage space vector by switching among the nearest voltage space vectors. SVPWM is considered a better technique of PWM owing to its advantages (i) improved fundamental output voltage (ii) reduced harmonic distortion (iii) easier implementation in microcontrollers and Digital Signal Processor. This paper considered the most popular structure among the transformer-less voltage source multilevel inverters, the diode-clamped converter based on the neutral point converter with SVPWM technique by Carrara et al. (1992). This paper proposes a single carrier multi-modulation technique for multilevel inverter driven induction machine, modeled in synchronously rotating reference frame. Simulation results present comparison of single and multicarrier SVPWM of nine-level diode-clamped inverter. Improved fundamental component of voltage is observed with SCMM method. Reduced total harmonic distortion and current ripple can be observed with Alternate Phase Opposition Disposition Carrier (APODC) SVPWM technique by Leon et al. (1999). Simulation is carried out in MATLAB-Simulink software.

2. Diode-Clamped Multilevel Inverter

A three-phase nine-level diode-clamped inverter is shown in Fig.1. Each phase is constituted by 16 switches. The complementary switch pairs for phase 'A' are (S_{a1}, S_{a1}'), (S_{a2}, S_{a2}'), (S_{a3}, S_{a3}'), (S_{a4}, S_{a4}'), (S_{a5}, S_{a5}'), (S_{a6}, S_{a6}'), (S_{a7}, S_{a7}'), (S_{a8}, S_{a8}') and similarly for B and C phases. Clamping diodes carry the full load current by Jose Rodriguez (2002).

Table1 shows phase to fictitious midpoint 'o' of capacitor string voltage (V_{AO}) and line-to-line voltage (V_{AB}) for various switching's.

Table 1 Nine-Level Inverter Voltage States

S_{a1}	S_{a2}	S_{a3}	S_{a4}	S_{a5}	S_{a6}	S_{a7}	S_{a8}	V_{AO}	V_{AB}
1	1	1	1	1	1	1	1	$+V_{dc}/2$	V_{dc}
0	1	1	1	1	1	1	1	$+3V_{dc}/8$	$7V_{dc}/8$
0	0	1	1	1	1	1	1	$+V_{dc}/4$	$6V_{dc}/8$
0	0	0	1	1	1	1	1	$+V_{dc}/8$	$5V_{dc}/8$
0	0	0	0	1	1	1	1	0	$5V_{dc}/8$
0	0	0	0	0	1	1	1	$-V_{dc}/8$	$3V_{dc}/8$
0	0	0	0	0	0	1	1	$-V_{dc}/4$	$2V_{dc}/8$
0	0	0	0	0	0	0	1	$-3V_{dc}/8$	$V_{dc}/8$
0	0	0	0	0	0	0	0	$-V_{dc}/2$	0

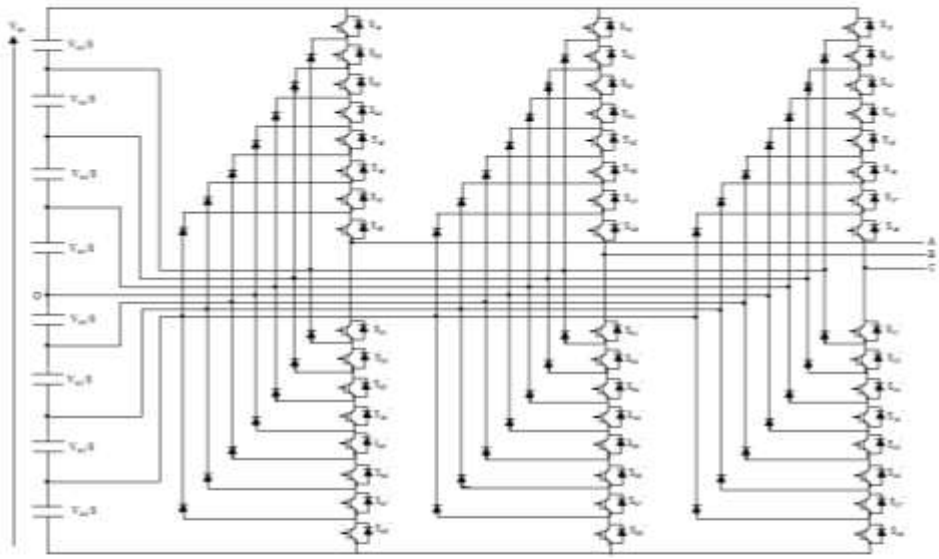

Figure 1 Circuit Diagram of 3 Phase Nine Level Diode Clamped Inverter

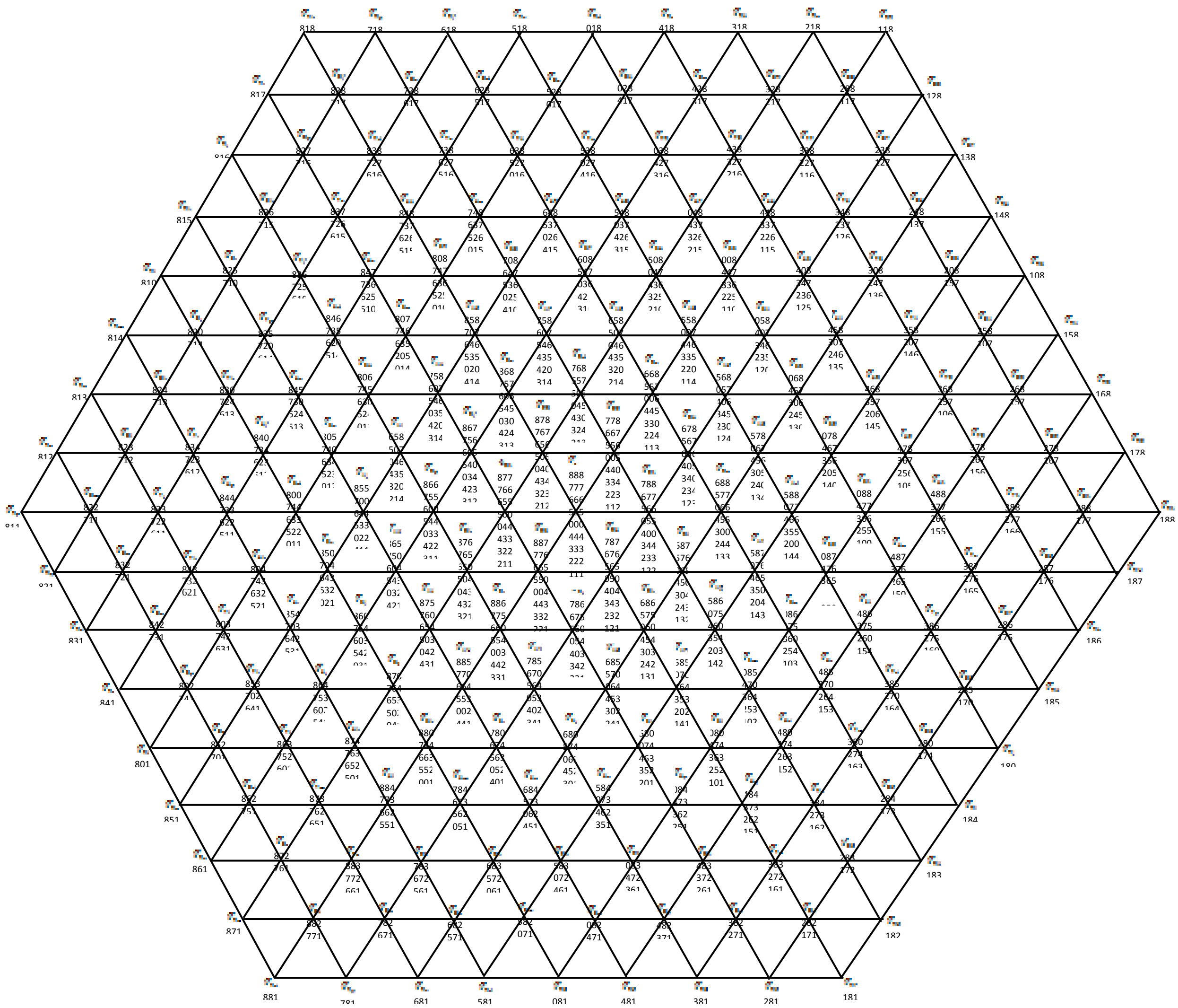

Figure 2 Nine-Level Inverter State Space Vector Diagram

3. SVPWM Implementation

Implementation of SVPWM involves (i) Sector identification-where the tip of the reference voltage vector lies (ii) Nearest three voltage space vectors (NTV) identification (ii) Determination of the dwelling time of each of these NTVs (iv) Choosing an optimized switching sequence.
Space vector diagram of nine-level inverter with its 729 ($=3^9$) vectors are shown in Fig 2. Each sector takes 60 degrees. Sector1 diagram is shown in Figure 3. Each sector consists of 64 regions 177 vectors.

3.1 Sector and Region identification

Three phase instantaneous reference voltages (1) are transformed to two phase (2). Every 60 degrees, from zero to 360 degrees constitute a sector. Identification of the sector in which the tip of the reference vector lies is obtained by (3).

$$V_a = V_m \sin \omega t$$

$$V_b = V_m \sin(\omega t - 2\pi/3) \qquad (1)$$

$$V_b = V_m \sin(\omega t - 4\pi/3)$$

$$V_\alpha = \frac{2}{3}\left(V_a - \frac{1}{2}(V_b + V_c)\right)$$

$$V_\beta = \frac{1}{\sqrt{3}}(-V_b + V_c) \tag{2}$$

$$V_{\text{ref}} = \sqrt{(V_\alpha)^2 + (V_\beta)^2} \quad ; \theta = \tan^{-1}(V_\beta/V_\alpha) \tag{3}$$

Where θ is the angle varies from 0 to 2π.

Amplitude and angle of the reference vector are obtained from (3).

From Park's transformation the di-phase, α-β components are:

$$K_1 = K_n.\left(\cos\theta - \frac{1}{\sqrt{3}}\sin\theta\right) \tag{4}$$

$$K_2 = K_n.\frac{\sin\theta}{\sin(\pi/3)} \tag{5}$$

Region is obtained by normalizing the di-phase components of the space vector (4)-(5) of an *n*-level inverter through division by V_{dc}/n-1, where V_{dc} is the dc link voltage.

3.2 Determination of the duration of nearest three voltage space vectors

Switch dwelling duration is obtained from (6)-(7).

$$T_s\vec{V}_{ref} = T_1\vec{V}_1 + T_2\vec{V}_2 + T_3\vec{V}_3 \tag{6}$$

$$T_s = T_1 + T_2 + T_3 \tag{7}$$

3.3 Determination of optimized switching sequence

Consider reference vector is lying in sector1 region 35 of Figure 3. The nearest three space vectors for switching sequence are $\vec{V}_{65}, \vec{V}_{66}, \vec{V}_{76}$.

The space redundant vectors for sector1-region 35, are, for $\vec{V}_{65}$ 4 0 8, 3 5 7, 2 3 6, 1 2 5 (4 redundant vectors), for $\vec{V}_{66}$ 4 4 8, 3 3 7, 2 2 6, 1 1 5 (4 redundant vectors), and for $\vec{V}_{76}$ 3 4 8, 2 3 7, 1 2 6 (3 redundant vectors).

An optimized switching sequence starts with virtual zero vector's state. A virtual zero vector is with minimum offset from zero vector of two-level inverter. Based on the principles derived in literature for two-level inverter, for Region 35, the switching sequence is 4 0 8→4 4 8→ 3 4 8→ 3 4 7→ 3 3 7→ 2 3 7→ 2 3 6→ 2 2 6→ 1 2 6→ 1 2 5→ 1 1 5 during a sampling interval and 1 1 5→ 1 2 5→ 1 2 6→ 2 2 6→ 2 3 6→ 2 3 7 → 3 3 7→ 3 4 7→ 3 4 8 → 4 4 8 → 4 0 8 during the subsequent sampling interval. This sequence uses all the space redundant vectors of each state by Anish Gopinath et al.(2007), (2009).

4. Mathematical Modeling of Induction Machine

Three-phase asynchronous or induction machines which contain a cage, are very popular motors in many industrial variable speed drive applications and all this is due to its simple construction, robustness, inexpensive, reliability, good efficiency and good self-starting capability and available at all power ratings. Progress in the field of power electronics and microelectronics enables the application of induction motors for high-performance drives, where traditionally only DC motors were applied. During starting up and other severe transient operations induction motor draws large currents, produces voltage dips, oscillatory torques and can even generate harmonics in the power systems by Vivek Pahwa et al.(2009), Ogubuka et al.(2009). It is important to predict these phenomena. A transient free operation of the induction machine is achieved only if the stator flux linkages are maintained constant in magnitude and its phase is stationary with respect to the current by Krishnan (2003) and Leon et al. (1999). Various models have been developed and the qd0 or two axis model for the study of transient behaviors has been tested and proved to be very reliable and accurate.

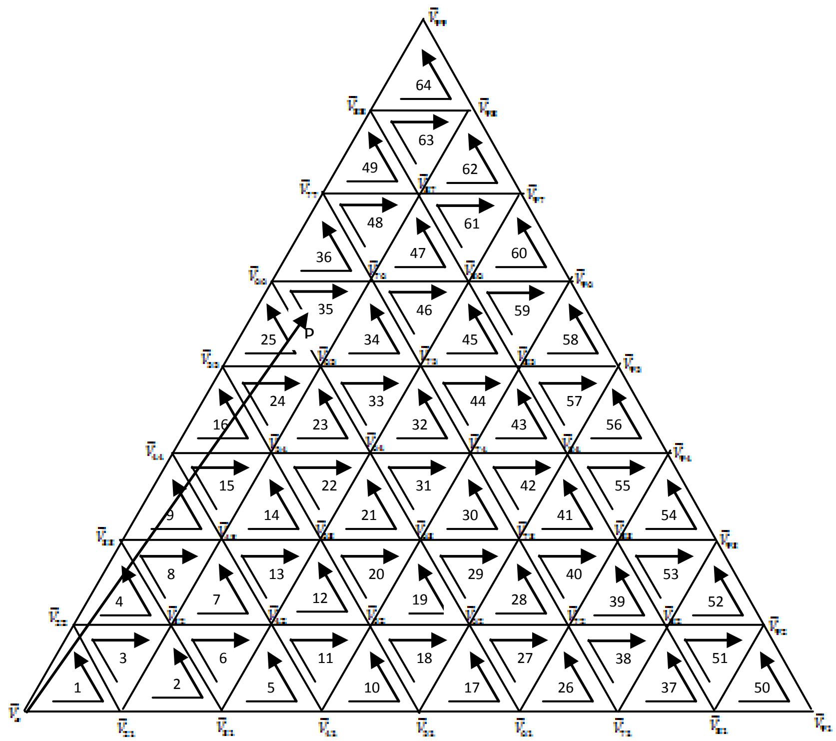

Figure 3 Sector1 Regions Space Vector Representation

4.1 Synchronously Rotating Reference Frames Model

The three phase balanced voltages are transformed to di-phase components which are in stationary rotating reference frame. These are transformed to synchronously rotating reference frames using (11). The speed of the synchronously rotating reference frames is the stator supply angular frequency.

$$v_{qds}^{e} = \left[T^{c}\right] v_{qds} \quad (8)$$

$$v_{qds}^{e} = \left[v_{qs}^{e} \quad v_{ds}^{e}\right]^{t}, \qquad v_{qds} = \left[v_{qs} \quad v_{ds}\right]^{t} \quad (9)$$

$$\left[T^{c}\right] = \begin{bmatrix} \cos\theta & -\sin\theta \\ \sin\theta & \cos\theta \end{bmatrix} \quad (11)$$

$$\begin{bmatrix} V_{qs}^e \\ V_{ds}^e \\ V_{qr}^e \\ V_{ds}^e \end{bmatrix} = \begin{bmatrix} R_s + L_s p & \omega_s L_s & L_m p & \omega_s L_m \\ -\omega_s L_s & R_s + L_s p & -\omega_s L_m & L_m p \\ L_m p & (\omega_s - \omega_r) L_m & R_r + L_r p & (\omega_s - \omega_r) L_r \\ -(\omega_s - \omega_r) L_m & L_m p & -(\omega_s - \omega_r) L_r & R_r + L_r p \end{bmatrix} \begin{bmatrix} i_{qs}^e \\ i_{ds}^e \\ i_{qr}^e \\ i_{ds}^e \end{bmatrix} \quad (13)$$

The electromagnetic torque is

$$T_e = \frac{3}{2}\frac{P}{2} L_m (i_{qs}^e i_{dr}^e - i_{qr}^e i_{ds}^e) \quad (14)$$

4.2 V/f Control on Induction Motor

Most of the industrial loads are operated based on constant Volts/Hz control method of speed because of its simplicity. Neglecting the stator resistance drop, the ratio of supply voltage to frequency is maintained constant by varying these variables. When the frequency approaches to zero, the magnitude of the stator voltage also tends to zero and the stator resistance absorbs this low voltage. The stator resistance drop is compensated at low speed by injecting the boost voltage to maintain rated air gap flux thus full load torque is available up to zero speed. At steady state operation, if load torque is increased, the slip increases within stability limit and a balance will be maintained between the developed torque and the load torque. This paper considered the V/f control on induction machine by Krishnan (2003).

5. Simulation Results and Conclusions

Simulation is carried out on nine-level diode-clamped inverter driven induction machine in synchronously rotating reference frame for two methods of Space Vector PWM technique at switching frequency 1.5 KHz with APODC technique.

(i) SCMM CSVPWM-Single Carrier Multi-Modulation for Conventional SVPWM
(ii) MCMM CSVPWM-Multi-Carrier Multi-Modulation for Conventional SVPWM

In MCMM the carriers are in Alternative phase opposition disposition, where each carrier band is shifted by 180^0 from the adjacent bands.

Multi-Carrier Multi-Modulation results reduced harmonic distortion with reduced fundamental component; however Single Carrier Multi-Modulation results reduced harmonic distortion with highly improved fundamental component of voltage.

Figure4 and Figure5 are responses of induction machine for stator currents, electromagnetic torque and speed of MCMM and SCMM respectively.

The response is observed for speed reversal from +314 rad/sec to -314 rad/sec at time of 0.86 seconds and from -314 rad/sec to +314 rad/sec at time of 0.85 seconds and 1.01 seconds respectively, in Figure6 and Figure7. Transients are more in MCMM compared to SCMM. Reduced oscillatory behavior is observed in MCMM. Settling time is less in SCMM compared to MCMM.

Figure6 shows the toque response with speed reversal at 0.86 seconds. When compared to MCMM, SCMM results more torque.

Figure7 shows the speed response with change in toque from 0 to 50 N-m at 0.4 seconds. When compared SCMM, dip in speed is more in MCMM.

Figure8 and Figure9 are the pole, phase and line voltages for SCMM and MCMM methods respectively.

Figure12 and Figure13 show the stator currents, torque and speed response for constant V/f control. The load torque requirement shifts from 0 to 50 N-m at 0.4 seconds. Modulation index is 0.906 (50 Hz) at 0 seconds, 0.84 (46 Hz) at 0.8 seconds, 0.73 (40 Hz) at 1.2 seconds, 0.62 (35 Hz) at 1.6 seconds, 0.906 (-50 Hz) at 2 seconds, 0.84 (-46 Hz) at 2.4 seconds, 0.73(-40 Hz) at 2.8 seconds, and 0.62 (-35 Hz), at 3.2 seconds.

Figure14 and Figure15 are the pole, phase and line voltages for SCMM and MCMM methods respectively for constant V/f control.

When frequency falls below 40 Hz the MCMM performance is poor compared to SCMM.

Ripple content is high with V/f control in SCMM.

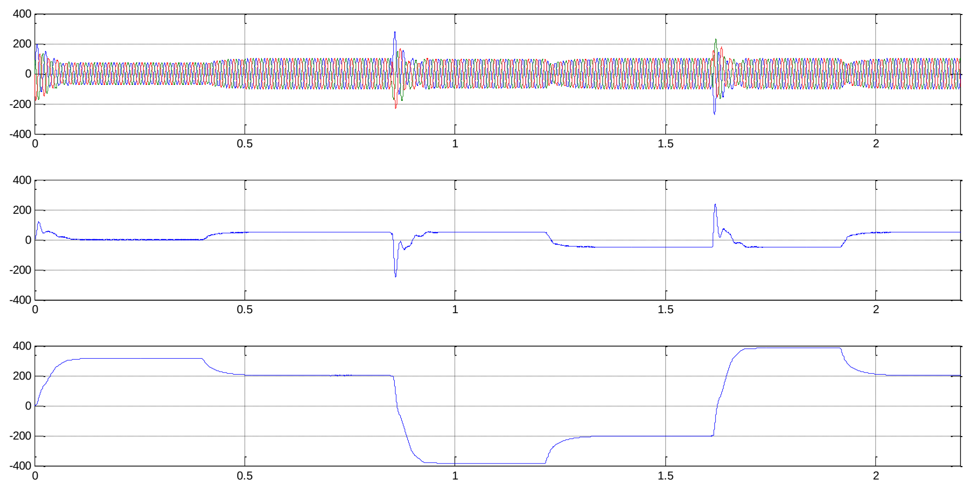

Figure 4 MCMM Stator Currents, Torque and Speed

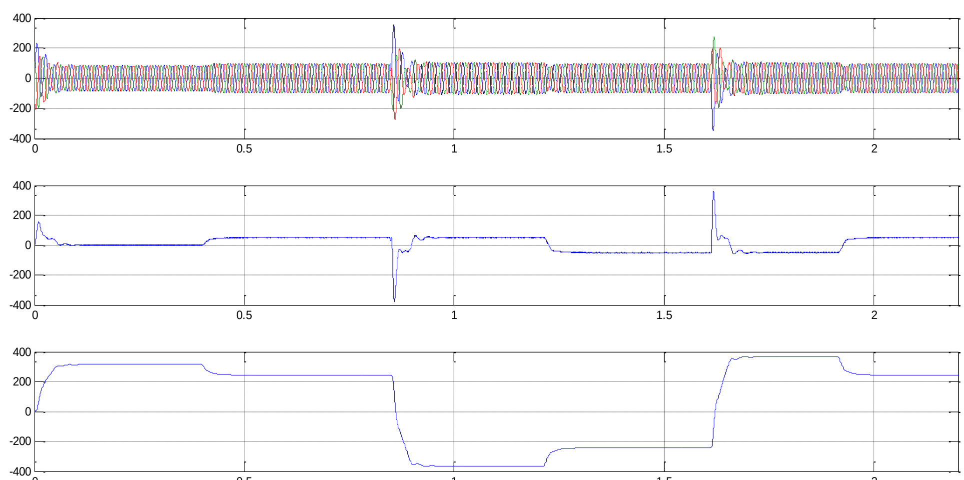

Figure 5 SCMM Stator Currents, Torque and Speed

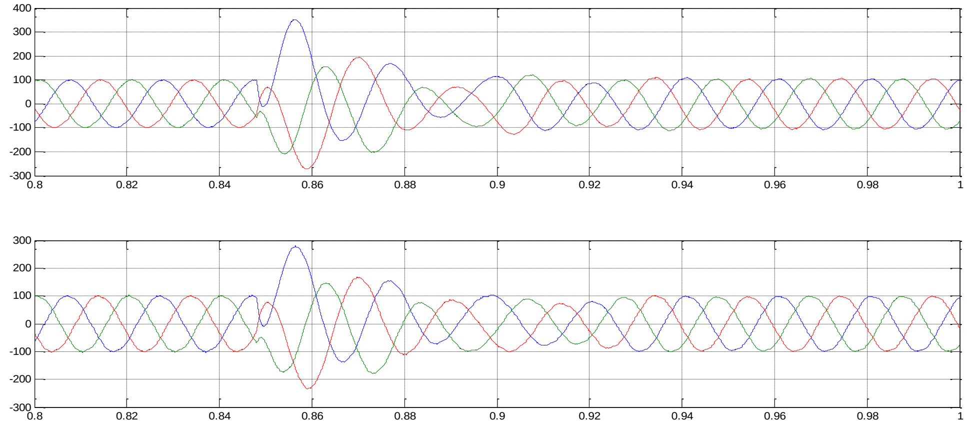

Figure 6 SCMM, MCMM Stator Currents for speed reversal from +314rad/sec to -314 rad/sec

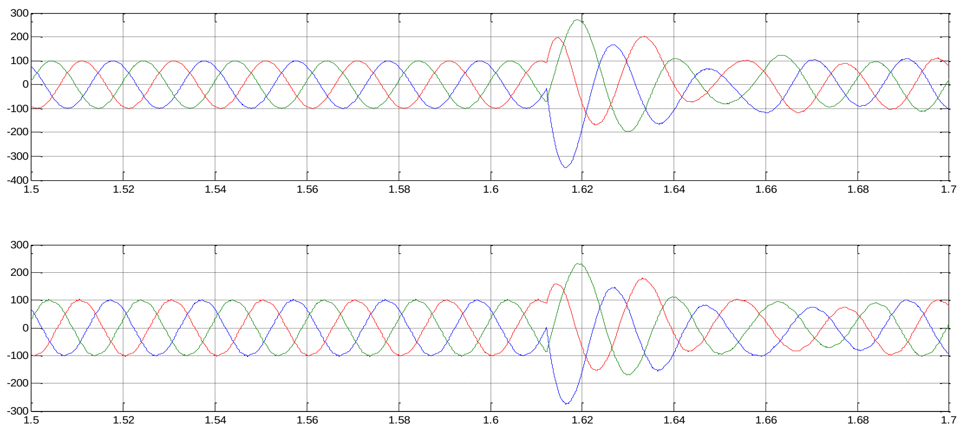

Figure 7 SCMM, MCMM Stator Currents for speed reversal from -314rad/sec to +314 rad/sec

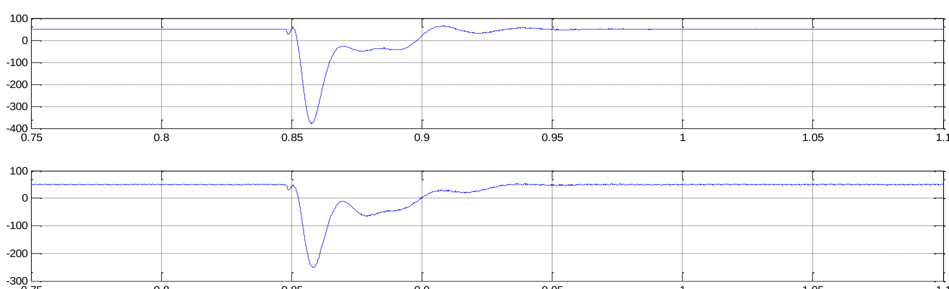

Figure 8 SCMM, MCMM Electromagnetic torque for speed reversal at 0.86sec

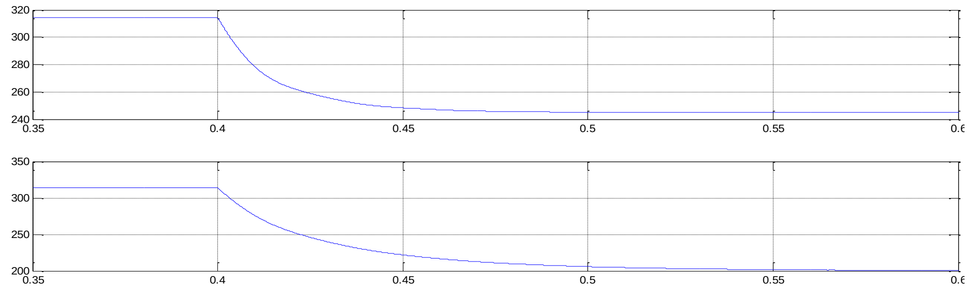

Figure 9 SCMM, MCMM rotor speed when torque change from 0 to +50 N-m

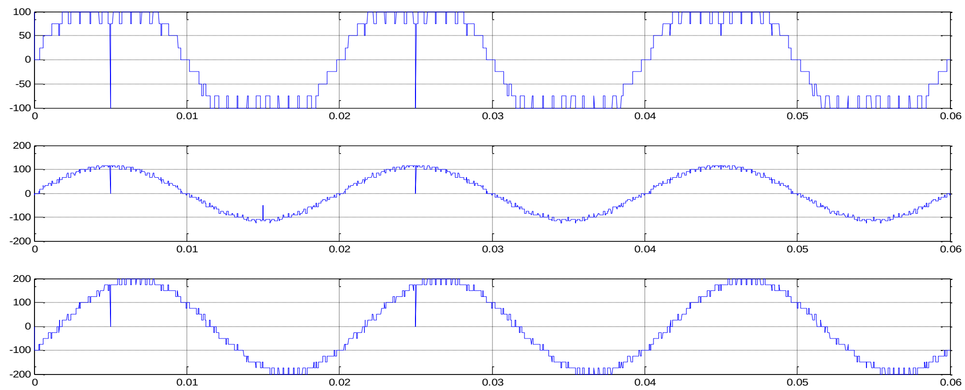

Figure 10 SCMM Pole, Phase and Line Voltage

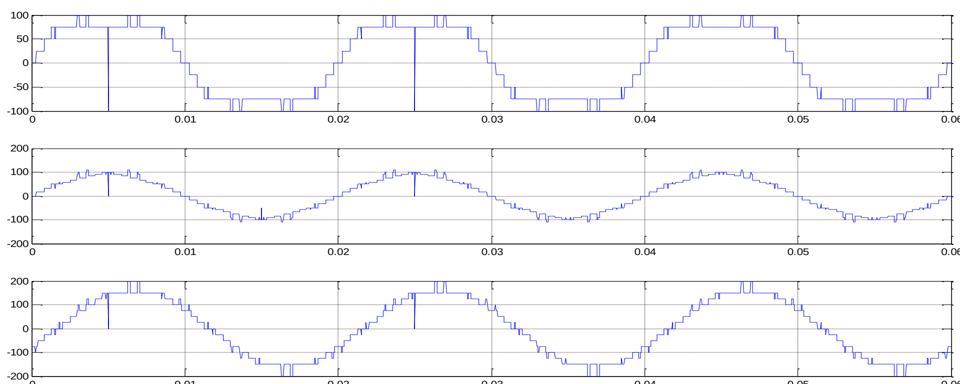

Figure 11 MCMM Pole, Phase and Line Voltage

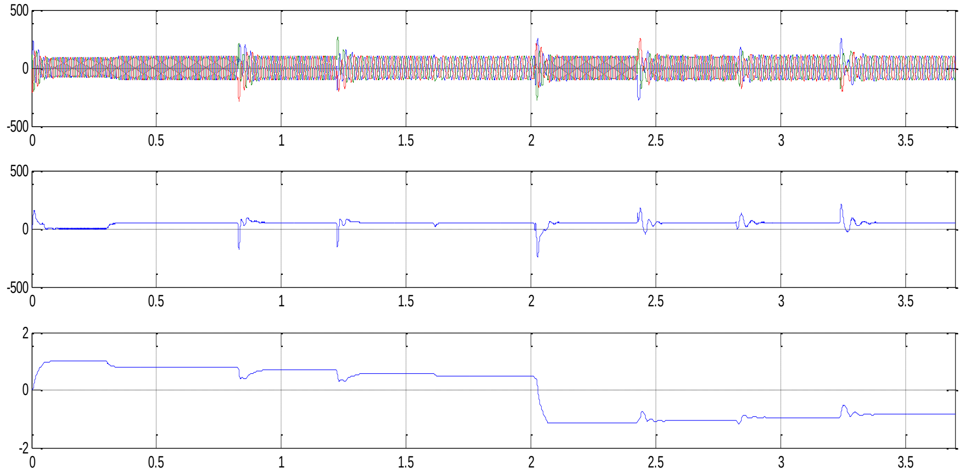

Figure 12 SCMM Stator Currents, Torque and Speed with V/f Control

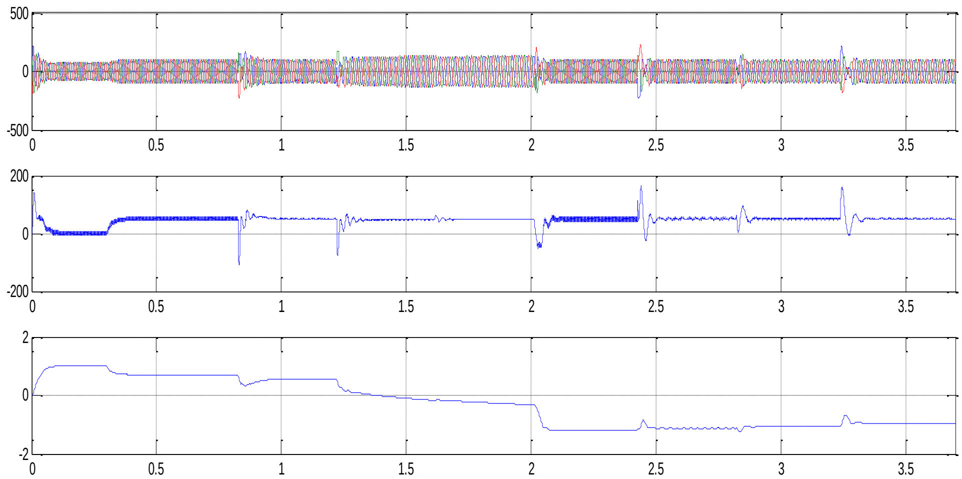

Figure 13 MCMM Stator Currents, Torque and Speed with V/f Control

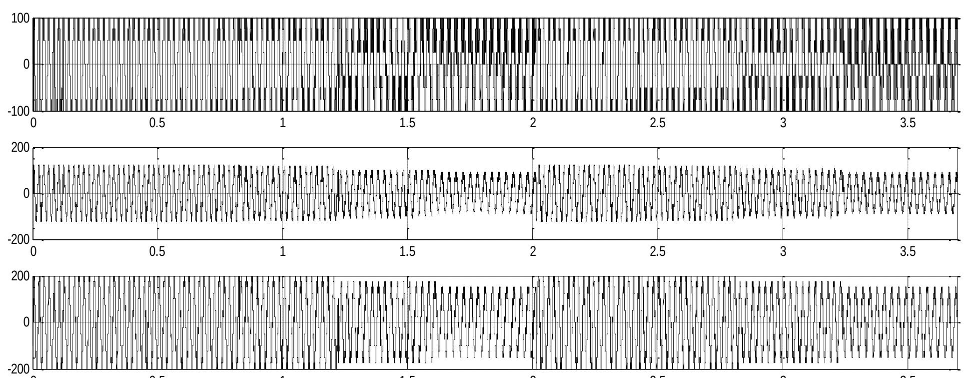

Figure 14 SCMM Pole, Phase and Line Voltages with V/f Control

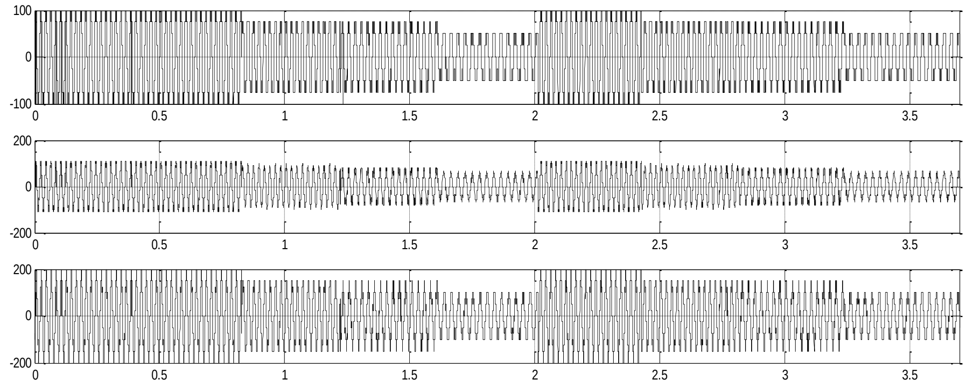

Figure 15 MCMM Pole, Phase and Line Voltages with V/f Control

4. References

Nabae, Takahashi, Akagi.(1981) "A Neutral-Point Clamped PWM inverter", IEEE Transactions on I.A., Vol. IA-17, No. 5, pp. 518-523.

Carrara, Gardella, Marchesoni, Salutari, and Sciutto, (1992) " A New Multilevel PWM Method: A theoretical Analysis", IEEE Transactions on Power Electronics, Vol. 7, No. 3, July, pp.497-505.

José Rodríguez, Jih-Sheng Lai, Fang Zheng Peng (2002) "Multilevel Inverters: A Survey of Topologies, Controls, and Applications", IEEE Trans., VOL. 49, NO. 4, AUGUST

Anish Gopinath, Baiju, (2007) "Space Vector PWM for Multilevel Inverters- A Fractal Approach" PEDS, Vol.56, No. 4, April, pp 1230-1237

Anish Gopinath, Aneesh Mohammed, and Baiju, (2009) "Fractal Based Space Vector PWM for Multilevel Inverters-A Novel Approach" IEEE Transactions on Industrial Electronics, Vol.56, No. 4, April, pp 1230-1237

Vivek pahwa, Sandhu (2009) "Transient Analysis of Three-phase Induction Machine using Different Reference Frames" ARPN Journal of Engineering and Applied Sciences, Vol. 4, No.8.

Ogabuka, Eng (2009) "Dynamic Modelling and Simulation of a 3-HP Asynchronous Motor Driving a Mechanical Load" The Pacific Journal of Science and Technology, Vol. 10, No. 2.

Krishnan (2003) "Electric Motor Drives" Pearson prentice Hall.

Leon Tolbert, Fang Peng, ,Thomas Habetler (1999) "Multilevel PWM Methods at Low Modulation Indices" APEC '99, Dallas, Texas, March 14-18, pp 1032-1039.